ELSEVIER

Inorganica Chimica Acta 264 (1997) 297–303

Inorganica Chimica Acta

Evidence of C–H activation of acetone by a platinum(II) complex. Synthesis and structural characterization of [Pt(CH_2COCH_3)Cl(bipy)] (bipy = 2,2′-bipyridyl)

Larry R. Falvello *, Raquel Garde, Eva M. Miqueleiz, Milagros Tomás *, Esteban P. Urriolabeitia

Departamento de Química Inorgánica, Instituto de Ciencia de Materiales de Aragón, Universidad de Zaragoza-CSIC, 50009 Zaragoza, Spain

Received 6 March 1997; revised 10 April 1997; accepted 2 June 1997

Abstract

Probable C–H activation of acetone under mild conditions by a neutral Pt(II) compound and the formation of the acetonyl complex [Pt(CH_2COCH_3)Cl(bipy)] (bipy = 2,2′-bipyridyl) (**1**) are reported. The complex [Pt(CH_2COCH_3)Cl(bipy)] has been characterized by IR and ^{1}H NMR spectroscopy, elemental (C, N and H) analysis and X-ray diffraction. Complex **1** crystallizes in the triclinic space group $P\bar{1}$: $a = 7.6599(9)$, $b = 9.157(2)$, $c = 9.306(1)$ Å, $\alpha = 87.581(8)°$, $\beta = 78.174(9)°$, $\gamma = 79.59(1)°$, $Z = 2$. The possible mechanism and some factors that influence the formation of this complex are discussed. © 1997 Elsevier Science S.A.

Keywords: C–H activation; Acetonyl complexes; Platinum complexes; Crystal structures

1. Introduction

C–H activation is an important step in many organic and biological reactions. C–H activation of acetone by some transition metal complexes is known, for instance, by chlororhodium(III) complexes of *trans*- and *cis*-5,15-bis(2-hydroxy-1-naphthyl)octaethylporphyrin [1], or by 2-phenylazophenylgold(III) complexes [2], or by porphyrins [3] or *N,N′*-ethylenebis(salicylideniminato) [4] derivatives of Co(II). Also, acetone C–H activation by the iridium complex Cp*(PMe$_3$)Ir(Me)(OTf) (Cp* = η^5-$C_5(CH_3)_5$, OTf = OSO_2CF_3) [5] and by the ruthenium complex [{Ru(AN)$_3$(TMP)$_2$}$_2$(μ-S_2)](CF$_3$SO$_3$)$_4$ (AN = NCCH$_3$, TMP = P(OMe)$_3$) [6] has recently been reported.

Although acetonyl derivatives of platinum(II) are known [7], they have been prepared only by reaction of hydroxoplatinum(II) derivatives, which behave as strong bases, with acetone. This method, using strong bases, is a well-known route for preparing metallated ketones. However, to our knowledge no C–H activation of acetone by a Pt(II) complex has yet been reported.

Scheme 1 shows the main steps in the intramolecular cooperative process proposed by Aoyama et al. [1] in which a weak Brønsted base and a Lewis acid can produce the C–H activation of acetone. This mechanism was used to explain the formation of the previously reported acetonylrhodium(III) [1] and gold(III) complexes [2]. According to this scheme, the metal complex must have: (1) an atom that can behave as a Brønsted base (atom B in Scheme 1); (2) the possibility of coordinating an acetone molecule; and (3) positioning of atom B (Brønsted base) in such a way that it can interact with an H atom of the acetone molecule. Condition (2) can be met a priori if the metal already has an empty orbital or a labile ligand. In order to labilize a ligand, a second ligand with a strong *trans* effect can be used. Conditions (1) and (2) are especially important in the formation of the aforementioned acetonyl gold(III) complexes.

Scheme 2 [2] shows the formation of a gold complex (intermediate **c**) that fulfills conditions (1), (2) and (3). The starting material, Cl$_2$Au(L–L′) (Scheme 2, molecule **a**), for the formation of acetonyl gold(III) complexes does not possess an empty coordination position at the metal atom (condition (2)), and there is no atom in a suitable position to act as a Brønsted base for the intramolecular cooperative process. As can be seen (Scheme 2), the empty coordination position can be obtained by weakening one of the bonds of the bidentate ligand (Au–N), for instance, by using a group X with a strong *trans* effect *trans* to the N atom (Scheme 2,

* Corresponding authors.

PII S0020-1693(97)05705-8

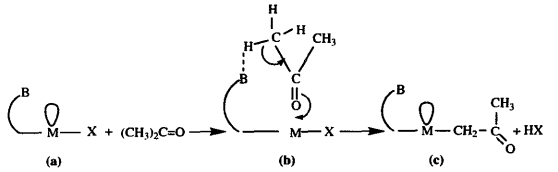

Scheme 1.

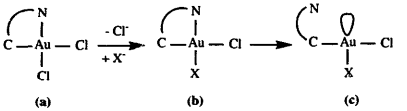

Scheme 2.

compound **b**). Then one of the original positions of the bidentate ligand, the spot vacated by the N atom (Scheme 2, intermediate **c**) can be used for coordinating the acetone molecule; and, depending on the topology of the LL′ ligand, the free donor atom (N in this case) can act as a Brønsted base. Vicente et al. [2] have found that the steps in Scheme 2 are especially important for C–H activation, since (L–L′)$AuCl_2$ does not react with acetone; and it is necessary to substitute one of the Cl atoms for another group with a stronger *trans* effect, such as C_6F_5, acac or $C_6H_3NO_2$, in order to obtain the acetonyl derivative.

We report here the formation of the complex [$Pt(CH_2COCH_3)Cl(bipy)$] (**1**) by way of C–H activation of acetone by a Pt(II) complex, probably through a similar intramolecular cooperative process. In this case, however, the formation of the active intermediate (Scheme 1, compound **a**, or Scheme 2, compound **c**) is obtained in a novel manner.

2. Experimental

Carbon, hydrogen and nitrogen analyses were carried out on a Perkin-Elmer 240-B or 2400 microanalyzer. IR spectra were recorded on a Perkin-Elmer 599 spectrophotometer (4000–200 cm^{-1}) from Nujol mulls between polyethylene sheets. ^1H NMR spectra were recorded at a measuring frequency of 300.13 MHz from $CDCl_3$, CD_2Cl_2 or $(CD_3)_2CO$ solutions at room temperature on a Bruker ARX-300 spectrometer. The spectra were referenced using the solvent signal as internal standard.

2.1. Preparation of *cis*-$Cl_2Pt(NCCH_3)_2$

Solid, finely ground $PtCl_2$ (1.50 g, 5.64 mmol) was stirred in neat $NCCH_3$ for 24 h at room temperature. After the reaction time, the remaining insoluble material was filtered off and identified spectroscopically as a mixture of $PtCl_2$, *trans*-$Cl_2Pt(NCCH_3)_2$ and *cis*-$Cl_2Pt(NCCH_3)_2$. The resulting yellow solution was evaporated to small volume (about 5 ml) and the pale yellow solid formed was filtered off and washed with 25 ml of an acetone/n-hexane (1/10) solution. The solid was identified by IR and NMR spectroscopy as *cis*-$Cl_2Pt(NCCH_3)_2$ (1.40 g). Yield: 71%. The preparation of this compound by another synthetic route has been reported previously [8].

2.2. Preparation of *trans*-$Cl_2Pt(NCCH_3)_2$

This compound was synthesized by isomerization of *cis*-$Cl_2Pt(NCCH_3)_2$ (0.400 g, 1.15 mmol), which was dissolved in neat $NCCH_3$ (40 ml) and kept at reflux temperature for 32 h. After cooling to room temperature, the solution was evaporated to small volume (about 10 ml), resulting in the precipitation of the insoluble *trans* isomer. The solid was identified by IR and NMR spectroscopy as *trans*-$Cl_2Pt(NCCH_3)_2$ and the isomerization was complete (0.36 g). Yield: 90%. The preparation of this compound by another synthetic route has been reported previously [8].

2.3. Reaction of *cis*-$Cl_2Pt(NCCH_3)_2$ with bipy at room temperature. Preparation of [$Pt(CH_2COCH_3)Cl(bipy)$] (1)

To an acetone solution (30 ml) of *cis*-$Cl_2Pt(NCCH_3)_2$ (0.080 g, 0.23 mmol) was added bipy (0.0360 g, 0.23 mmol). After 15 days of stirring at room temperature, the yellow precipitate was filtered off and identified as the complex [$Pt(CH_2COCH_3)Cl(bipy)$] (**1**, 0.021 g). Yield: 21%. The acetone solution was evaporated to dryness and the residue was treated with 40 ml of a mixture of $CHCl_3$/n-hexane (1/6) to give a red solid. The IR spectrum of the latter indicated (see Table 2) that it was a mixture of two compounds: *cis*-$Cl_2Pt(NCCH_3)_2$ and the red form of Cl_2Pt(bipy). During an attempt to separate the components of the red solid, a few crystals of the red form of Cl_2Pt(bipy) were obtained. They were characterized by X-ray diffraction, which gave the unit cell $a=17.641(2)$, $b=9.076(1)$, $c=6.803(1)$ Å, $\alpha=90°$, $\beta=90°$, $\gamma=90°$ [9].

Anal. Calc. for $C_{13}H_{13}ClN_2OPt$ (MW 443.8): C, 35.17; H, 2.93; N, 6.31. Found: C, 34.73; H, 2.65; N, 6.30%. IR (ν, cm^{-1}): 1639 (s, ν_{CO}), 1608 (m, bipy), 1239 (s, bipy), 760 (s, bipy), 340 (s, ν_{Pt-Cl}). ^1H NMR ($CDCl_3$) δ: 2.31 (s, 3H, CH_3, $^4J_{Pt-H}=12.8$ Hz), 3.40 (s, 2H, CH_2, $^2J_{Pt-H}=109.5$ Hz), 7.58 (m, 2H, $H_3+H_{3'}$), 7.96 (m, 2H, $H_5+H_{5'}$), 8.09 (m, 2H, $H_4+H_{4'}$), 9.66, 9.88 (2d, 2H, $H_2+H_{2'}$, $^3J_{H_2-H_3}\cong$

$^3J_{H_2-H_Y} = 6$ Hz). This complex was insufficiently soluble for $^{13}C\{^1H\}$ NMR measurements, even in CD_2Cl_2.

2.4. Reaction of trans-$Cl_2Pt(NCCH_3)_2$ and bipy at room temperature

To an acetone solution (30 ml) of *trans*-$Cl_2Pt(NCCH_3)_2$ (0.200 g, 0.57 mmol) was added bipy (0.090 g, 0.57 mmol). After 8 days of stirring, the yellow precipitate was filtered off and identified by IR spectroscopy as *trans*-$Cl_2Pt(NCCH_3)_2$ (0.143 g). The yellow solution was evaporated to dryness and was treated with 20 ml of n-hexane to give an orange solid (0.03 g) whose IR spectrum indicated that it was a mixture of three complexes: $[Pt(CH_2COCH_3)Cl(bipy)]$ (**1**), the red form of $Cl_2Pt(bipy)$ and the starting material, *trans*-$Cl_2Pt(NCCH_3)_2$.

2.5. Reaction of cis-$Cl_2Pt(NCCH_3)_2$ and bipy at reflux temperature

To an acetone solution (30 ml) of *cis*-$Cl_2Pt(NCCH_3)_2$ (0.15 g, 0.43 mmol) was added bipy (0.067 g, 0.43 mmol) and the mixture was refluxed for 40 h. After cooling to room temperature, the yellow precipitate was filtered and identified spectroscopically as the yellow form of $Cl_2Pt(bipy)$ [9] (0.13 g). Yield: 71%. The yellow solution was evaporated to dryness and the residue treated with 20 ml of n-hexane giving 0.022 g of an orange solid identified spectroscopically as a mixture of three complexes: *trans*-$PtCl_2(NCCH_3)_2$, $[PtCl(CH_2COCH_3)(bipy)]$ and the red form of $Cl_2Pt(bipy)$.

2.6. Reaction of trans-$Cl_2Pt(NCCH_3)_2$ and bipy at reflux temperature

To an acetone solution of *trans*-$Cl_2Pt(NCCH_3)_2$ (0.090 g, 0.26 mmol) was added bipy (0.040 g, 0.26 mmol) and the solution was refluxed for 32 h. After cooling to room temperature, a beige precipitate was filtered off and identified as unreacted *trans*-$Cl_2Pt(NCCH_3)_2$ (0.042 g). The yellow solution was evaporated to dryness and the residue treated with 20 ml of n-hexane to give an orange solid identified by IR spectroscopy as a mixture of three compounds: *trans*-$Cl_2Pt(NCCH_3)_2$, $[Pt(CH_2COCH_3)Cl(bipy)]$ (**1**), and the red form of $Cl_2Pt(bipy)$.

2.7. X-ray crystallography

Diffraction data were measured on an automated four-circle diffractometer with PC control [10]. After initial indexing of the cell, which was based on 25 reflections located in a random search, the lattice parameters were checked by axial photography. Optimum scan parameters for intensity data collection were derived from two-dimensional (ω–θ) scans of 14 reflections. During data collection, a variable scan speed was used in which the weakest reflections were scanned for the longest time; that is, no reflection was skipped because of low intensity. Three monitor reflections were measured every 3 h as a check on experimental stability. The orientation of the crystal was checked after every 400 data points. Azimuthal scans of 9 scattering vectors, with bisecting-position χ values ranging from 26 to about 90° were used as the basis of a laminar absorption correction [11]. The structure was solved by an automated procedure that incorporates Patterson analysis, difference direct methods, and Fourier peak-list optimization and refined to all positive F_o^2 using full-matrix least-squares [12]. The hydrogen atoms of the methyl group at C(13) were located in a local slant Fourier calculation and treated as riding atoms with displacement parameters assigned as 1.5 times the equivalent isotropic displacement parameter of C(13). Although most of the remainder of the hydrogen atoms, including one of the two attached to the methylene carbon of the acetonyl ligand, were seen in difference Fourier maps, for the final refinement all the non-methyl hydrogen atoms were placed at calculated positions and treated as riding atoms, with displacement parameters assigned as 1.2 times the equivalent isotropic displacement parameters of their respective parent carbon atoms. The data-to-parameter ratio in the final refinement was 15:1. Least-squares residuals and other crystallographic parameters are summarized in Table 1. The larger-than-normal residual electron density located near the platinum atom can be attributed to remaining uncorrected absorption; the crystal was a thin plate and possessed a large linear absorption coefficient.

3. Results and discussion

During attempts to synthesize $Cl_2Pt(bipy)$ by a slow, room temperature reaction, we found that the reaction of *cis*-$[Cl_2Pt(NCCH_3)_2]$ with bipy in acetone produces, after stirring for 15 days at room temperature, the acetonyl complex $[Pt(CH_2COCH_3)Cl(bipy)]$ (**1**, 21% yield):

$$\textit{cis}\text{-}[Cl_2Pt(NCCH_3)_2] + bipy \rightarrow [Pt(CH_2COCH_3)Cl(bipy)]\ (\mathbf{1}) + Cl_2Pt(bipy) + [H(bipy)]Cl + 2NCCH_3 \quad (1)$$

The reaction also produces the complex $Cl_2Pt(bipy)$ which is isolated as the red form [9]. Although in this case it is reasonable to presume that HCl or $[H(bipy)]Cl$ (since there is free bipy ligand) is formed in the reaction, their presence has not been detected. However, it is interesting to note that $Cl_2Pt(bipy)$ is usually isolated as the yellow form and that the reported preparations of the red form contain HCl. Some starting material, *cis*-$[Cl_2Pt(NCCH_3)_2]$, was also recovered from the present preparation.

The acetonyl complex **1** has been characterized by its C, H and N analytical data, and by IR and ^1H NMR spectroscopy. The elemental analyses of **1** are in good agreement with the stoichiometry $[Pt(CH_2COMe)Cl(bipy)]$ (see Section 2),

Table 1
Crystal data for [Pt(CH$_2$COCH$_3$)Cl(bipy)] (**1**)

Formula	$C_{13}H_{13}ClN_2OPt$
Formula weight	443.79
Space group	$P\bar{1}$
Crystal system	triclinic
Systematic absences	none
a (Å)	7.6599(9)
b (Å)	9.157(2)
c (Å)	9.306(1)
α (°)	87.581(8)
β (°)	78.174(9)
γ (°)	79.59(1)
V (Å^3)	628.3(1)
Z	2
d_{calc} (g/cm^3)	2.346
Crystal size (mm)	0.22×0.12×0.04
μ (cm^{-1})	113.7
Transmission factors, max., min.	0.800, 0.331
Data collection instrument	Nonius CAD-4
Radiation (graphite monochromated)	Mo Kα ($\lambda_{(\alpha)}$ = 0.71073 Å)
Orientation reflections: no., range (2θ) (°)	25, 24.1–31.4
T (°C)	−123 (1)
Scan method	ω-scans
Data collection range, 2θ (°)	4.0–55.0
No. unique reflections	2598
No. reflections with $I > 2\sigma(I)$	2127
No. variables/restraints	163/0
$R1$ [a]	0.0496
$wR2$ [b]	0.1218
Weighting parameters g_1, g_2 [c]	0.0750, 0.00
Quality of fit [d]	1.003
Mean, max. shift/e.s.d., final cycle	<0.001, 0.003
Res. electron density (e/Å^3)	+2.76, −3.13

[a] $R1 = \Sigma \| F_o | - | F_c \| / \Sigma | F_o |$.
[b] $wR2 = [\Sigma w(F_o^2 - F_c^2)^2 / \Sigma w(F_o^2)^2]^{1/2}$.
[c] $w = [\sigma^2(F_o^2) + (g_1 P)^2 + g_2 P]^{-1}$; $P = [\max(F_o^2; 0) + 2F_c^2]/3$.
[d] Quality of fit = $[\Sigma w(F_o^2 - F_c^2)^2 / (N_{obs} - N_{param})]^{1/2}$.

while other possible stoichiometries such as [PtCl(NH$_2$COMe)(bipy)] or [Pt(NHCOMe)Cl(bipy)], which could be the result of hydrolysis processes on the acetonitrile ligand, do not correspond to the experimental values. The IR spectrum of **1** shows the following relevant absorptions: 1639 (s), 1607 (m), 760 (s) and 340 cm^{-1} (m). The absorption at 1639 cm^{-1} corresponds to the ν(C=O) stretching mode. This value falls in the range of the ν(C=O) absorptions found in other related platinum–acetonyl compounds [7] obtained from hydroxoplatinum complexes, *cis*-[Pt(CH$_2$COMe)Me(PPh$_3$)$_2$] (1650 cm^{-1}), *trans*-[Pt(CH$_2$COMe)Ph(PPh$_3$)$_2$] (1641 cm^{-1}) and [Pt(CH$_2$COMe)Ph(PEt$_3$)$_2$] (1625 cm^{-1}). The absorptions at 1607 and 760 cm^{-1} correspond to the bipy ligand, and the ν(Pt–Cl) absorption appears at 340 cm^{-1}. It is interesting to note that no absorptions are found in the ν(NH) region, precluding the existence of [PtCl(NH$_2$COMe)(bipy)] or [Pt(NHCOMe)Cl(bipy)], in agreement with the analytical results. Table 2 collects the IR absorptions of the acetonyl complex **1** together with other relevant IR absorptions of the *cis*- and *trans*-[Cl$_2$Pt(NCCH$_3$)$_2$] complexes and the Cl$_2$Pt(bipy) (yellow and red forms). Since all of these species present similar low solubilities, IR spectroscopy proved to be a useful tool in the identification of these compounds when mixtures were obtained.

The ^{1}H NMR spectrum of **1** shows the presence, in the high field region, of a singlet resonance at 3.40 ppm, flanked by ^{195}Pt satellites with a coupling constant of 109.5 Hz, attributed to the methylene protons of the Pt–C*H*$_2$ group. This chemical shift appears at lower fields than those reported for other related Pt–acetonyl complexes [7], which range from 2.12 to 2.43 ppm, probably due to the different nature of the *trans* substituents (phosphine versus bipyridyl). However, the value of the coupling constant $^2J_{Pt-H}$ (109.5 Hz) is fairly typical for Pt–C–*H* groupings [7,13] with a σ(Pt–C) bond. In addition, a singlet resonance appears at 2.31 ppm, also with ^{195}Pt satellites, attributed to the methyl group of the acetonyl ligand. Finally, in the low field region, eight complex resonances appear (some of them partially overlapped) corresponding to the eight chemically inequivalent aromatic protons of the 2,2′-bipyridyl ligand. The ^{13}C NMR of complex **1** was not studied because of the low solubility of the compound.

The crystal structure of [Pt(CH$_2$COCH$_3$)Cl(bipy)] (**1**) provides further characterization. A drawing of this organometallic complex is shown in Fig. 1, selected bond distances and angles are collected in Table 3 and atomic coordinates are collected in Table 4. The platinum atom is coordinated by the bipy ligand through the two nitrogen atoms, N(1) and N(2), by a chlorine atom, Cl(1), and by the acetonyl ligand through the methylene carbon C(11). The Pt–N bond distances are Pt(1)–N(1), 2.017 (9) Å and Pt(1)–N(2), 2.082 (11) Å. The longer distance corresponds to the Pt–N bond *trans* to the acetonyl ligand, while the shorter corresponds to the Pt–N bond *trans* to the chlorine atom. The slight difference observed is due to the stronger *trans* influence of the C atom versus the Cl atom. The Pt(1)–C(11) distance of 2.082

Table 2
Relevant IR absorptions (cm^{-1}) of compound **1** and related complexes

Complex	ν(C≡N)	bipy	ν(C=O)	ν(Cl–Pt)
cis-[Cl$_2$Pt(NCCH$_3$)$_2$]	2333 (m), 1031 (s)			363 (s), 354 (s)
trans-[Cl$_2$Pt(NCCH$_3$)$_2$]	2342 (m), 1020 (s)			351 (s)
Cl$_2$Pt(bipy) (yellow form)		1608 (m), 799 (w), 760 (s)		352 (s), 339 (s)
Cl$_2$Pt(bipy) (red form)		1617 (m), 799 (w), 760 (s)		340 (s)
[Pt(CH$_2$COCH$_3$)Cl(bipy)] (**1**)		1608 (m), 780 (w), 760 (s)	1639 (s)	340 (s)

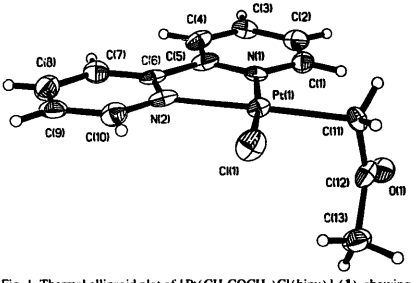

Fig. 1. Thermal ellipsoid plot of $[Pt(CH_2COCH_3)Cl(bipy)]$ (**1**), showing the atom labeling scheme. Non-hydrogen atoms are represented by their 50% probability ellipsoids.

Table 3
Selected bond lengths (Å) and angles (°) for $[Pt(CH_2COCH_3)Cl(bipy)]$ (**1**)

Pt(1)–N(1)	2.017(9)	O(1)–C(12)	1.238(14)
Pt(1)–C(11)	2.082(11)	C(11)–C(12)	1.47(2)
Pt(1)–N(2)	2.082(11)	C(12)–C(13)	1.50(2)
Pt(1)–Cl(1)	2.292(3)		
N(1)–Pt(1)–C(11)	97.4(4)	N(1)–Pt(1)–N(2)	79.0(4)
C(11)–Pt(1)–N(2)	175.5(4)	N(1)–Pt(1)–Cl(1)	173.2(3)
C(11)–Pt(1)–Cl(1)	88.6(3)	N(2)–Pt(1)–Cl(1)	95.1(3)
Pt(1)–C(11)–C(12)	104.1(8)	C(11)–C(12)–O(1)	122.6(11)
C(11)–C(12)–C(13)	120.1(10)	O(1)–C(12)–C(13)	117.3 (12)

Table 4
Atomic coordinates ($\times 10^4$) and equivalent isotropic displacement parameters ($Å^2 \times 10^3$) and their estimated standard deviations for $[Pt(CH_2COCH_3)Cl(bipy)]$ [a]

	x	y	z	U_{eq}
Pt(1)	2550(1)	3196(1)	3018(1)	21(1)
Cl(1)	1634(5)	2838(4)	884(3)	34(1)
O(1)	6727(12)	793(11)	3387(9)	32(2)
N(1)	3100(12)	3707(11)	4947(9)	21(2)
N(2)	1533(13)	5464(13)	3129(10)	28(2)
C(1)	3914(15)	2701(15)	5843(13)	27(2)
C(2)	4170(17)	3113(16)	7173(12)	31(3)
C(3)	3610(17)	4582(15)	7640(12)	27(3)
C(4)	2807(15)	5594(15)	6685(13)	29(3)
C(5)	2577(15)	5089(16)	5379(12)	28(3)
C(6)	1757(15)	6115(15)	4331(12)	25(2)
C(7)	1248(16)	7644(15)	4532(13)	28(3)
C(8)	475(18)	8473(16)	3456(14)	34(3)
C(9)	222(16)	7788(16)	2249(12)	30(3)
C(10)	761(16)	6279(15)	2110(12)	28(3)
C(11)	3735(16)	961(12)	2980(11)	21(2)
C(12)	5682(17)	973(14)	2516(13)	30(3)
C(13)	6486(18)	1195(16)	924(13)	35(3)

[a] The equivalent isotropic displacement parameter, U_{eq}, is calculated as: $U_{eq} = (1/3)\sum_{ij} U_{ij} a_i \cdot a_j a_i^* a_j^*$.

(11) Å and the Pt(1)–Cl(1) distance of 2.292 (3) Å are also typical of these kinds of bonds. The angle N(1)–Pt(1)–N(2) is acute (79.0(4)°), a typical value for the chelate angle

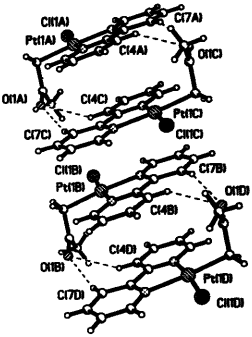

Fig. 2. Packing diagram of $[Pt(CH_2COCH_3)Cl(bipy)]$ (**1**), showing the hydrogen bonding interactions between molecules.

of the bipy ligand. The C=O distance in the acetonyl ligand is 1.238 (14) Å. Distances similar to this have been observed for C=O bonds of acetonyl groups [3,14,15]. All the atoms of the molecule are nearly coplanar, except the $COCH_3$ atoms of the acetonyl group. The atoms that deviate most from the best least-squares plane of the remaining atoms are Cl(1) (−0.152 (6) Å) and C(11) (0.149 (8) Å) (r.m.s. deviation of fitted atoms is 0.068). The molecules pack in such a way that all the molecular planes are parallel to each other as required by the center of symmetry (space group $P\bar{1}$) and in accord with the fact that there are only two molecules per unit cell ($Z=2$).

Fig. 2 shows some features of the molecular packing. There are hydrogen bonds between the oxygen atom, O(1A), of the carbonyl group of one molecule and two hydrogen atoms of the bypyridine ligand (C(4C) and C(7C)) of another. Table 5 collects the main distances and angles for the atoms involved in these hydrogen bonds. Since the two molecules that interact in this way are related by a center of symmetry, there are another two hydrogen bonds related to these by the same symmetry element, O(1C)···H–C(4A) and O(1C)···H–C(7A) in Fig. 2. Thus, the molecules interact pairwise through four hydrogen bonds, forming dimers in the crystal. As just mentioned, the C(11)Cl(1)Pt(bipy) fragment of the molecule is planar, and parallel to the analogous fragments of the other molecules in the crystal. The distance between these planes in the pair of molecules that interact through hydrogen bonds is 3.33 Å. The shortest distance between the planes of the closest molecules that do not interact by hydrogen bonding is 3.74 Å. The short distance of 3.33 Å is similar to the distance between layers in graphite (3.35 Å) [16].

The formation of complex **1** is probably achieved by an intramolecular cooperative process similar to the one in Scheme 1. However, for the platinum complex, the active intermediate (Scheme 1, complex **a**, and Scheme 2, complex **c**) must be formed in a process different from the one shown

Table 5
Hydrogen-bond geometry in the crystal structure of [Pt(CH_2COCH_3)Cl(bipy)] (**1**)

Donor–H···acceptor	d(D···A) (Å)	d(H···A) (Å)	Angle(D–H···A) (°)	A coordinates
C(4)–H(4A)···O(1)	3.39(2)	2.56(2)	145.4(3)	1−x, 1−y, 1−z
C(7)–H(7A)···O(1)	3.24(2)	2.38(2)	150.5(4)	1−x, 1−y, 1−z

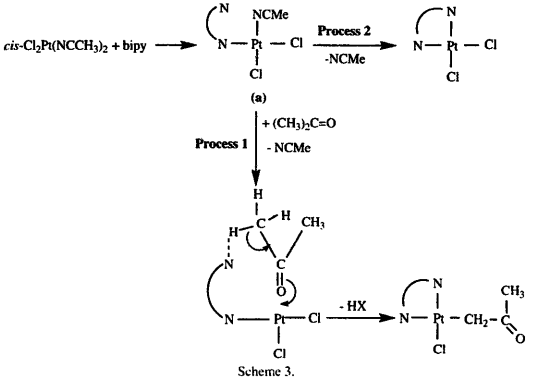

Scheme 3.

in Scheme 2. Scheme 3 shows some of the possible steps in the formation of this intermediate. Since there is bipy present, it is reasonable to propose that the active species has the bipy ligand coordinated just through one nitrogen; it is then the second N atom, the one that is not coordinated to platinum, which behaves as a Brønsted base (Scheme 3, complex **a**). This species is formed by the reaction of *cis*-[Cl_2Pt-($NCCH_3$)$_2$] with the bipy ligand and can be thought of as one of the first steps in the formation of Cl_2Pt(bipy) (Scheme 3, Process 2). In fact, the formation of Cl_2Pt(bipy) should be a competing process; and this can explain the 21% yield in the preparation of the acetonyl complex (Scheme 3, Process 1).

In this case, although the metal compound contains two Cl atoms, it is not necessary to replace one of them by a ligand with a strong *trans* effect in order to labilize one of the platinum–ligand bonds, since the second Pt–N(bipy) bond is not yet formed and the Pt–N(acetonitrile) bond is labile. However, as was just pointed out, the formation of the second Pt–N(bipy) bond is a competitive process that lowers the yield of the acetonyl complex.

Since starting material is recovered after stirring for 15 days at room temperature, the reaction of *cis*-Cl_2Pt($NCCH_3$)$_2$ with bipy in acetone was carried out at reflux temperature (40 h). Under these conditions, the solid formed is the yellow Cl_2Pt(bipy) (72% yield). Therefore, the higher temperature favors Process 2 over Process 1.

The reactions of *trans*-Cl_2Pt($NCCH_3$)$_2$ and bipy at room temperature and at acetone reflux temperature have also been carried out. In both cases, starting material is recovered; and from the acetone solutions a red solid that is a mixture of the acetonyl complex [Pt(CH_2COCH_3)Cl(bipy)] (**1**), the starting material *trans*-Cl_2Pt($NCCH_3$)$_2$ and Cl_2Pt(bipy) (red form) is obtained. These compounds have been identified on the basis of their IR spectra. Thus (Table 2), the compound *cis*-Cl_2Pt($NCCH_3$)$_2$ is the only one that presents absorptions at 2333 and 363 cm^{-1}, while *trans*-Cl_2Pt($NCCH_3$)$_2$ is the only one that presents an absorption at 2342 cm^{-1}. The strong absorption at 1639 cm^{-1} is the most important band since only the acetonyl compound gives it (ν(C=O)). The absorption at 1617 cm^{-1} is indicative of the presence of the red form of Cl_2Pt(bipy), while the absorption at 1608 cm^{-1} together with an absorption at 352 cm^{-1} indicates the presence of the yellow form of Cl_2Pt(bipy). Therefore, the *trans*-isomer can also produce the C–H activation of the acetone, although the reaction with the *cis*-isomer at room temperature produces the pure compound, and in better yield.

4. Supplementary material

For the crystal structure of compound **1**, tables of calculated and observed structure factors, hydrogen positions, bond distances and angles and anisotropic displacement parameters may be obtained from the authors upon request.

Acknowledgements

Funding by the Dirección General de Enseñanza Superior (Spain) under Grant PB95-0792 is gratefully acknowledged.

References

[1] Y. Aoyama, A. Yamagishi, Y. Tanaka, H. Toi and H. Ogoshi, *J. Am. Chem. Soc., 109* (1987) 4735.

[2] (a) J. Vicente, M.D. Bermudez, M.T. Chicote and M.J. Sanchez-Santano, *J. Chem. Soc., Chem. Commun.*, (1989) 141; (b) J. Vicente, M.D. Bermudez, M.T. Chicote and M.J. Sanchez-Santano, *J. Chem. Soc., Dalton Trans.*, (1990) 1945; (c) J. Vicente, M.D. Bermudez, J. Escribano, M.P. Carrillo and P.G. Jones, *J. Chem. Soc., Dalton Trans.*, (1990) 3083.

[3] M.E. Kastner and W.R. Scheidt, *J. Organomet. Chem., 157* (1978) 109.

[4] W.P. Schaefer, R. Waltzman and B.T. Huie, *J. Am. Chem. Soc., 100* (1978) 5063.

[5] B.A. Arndtsen and R.G. Bergman, *J. Organomet. Chem., 504* (1995) 143.

[6] K. Matsumoto, H. Uemura and M. Kawano, *Inorg. Chem., 34* (1995) 658.

[7] D.P. Arnold and M.A. Bennett, *J. Organomet. Chem., 199* (1980) 119, and Refs. therein.

[8] F.P. Fanizzi, F.P. Intini, L. Maresca and G. Natile, *J. Chem. Soc., Dalton Trans.*, (1990) 199.

[9] (a) R.S. Osborn and D. Rogers, *J. Chem. Soc., Dalton Trans.*, (1974) 1002; (b) E. Bielli, P.M. Gidney, R.D. Gillard and B.T. Heaton, *J. Chem. Soc., Dalton Trans.*, (1974) 2133, and Refs. therein.

[10] Diffractometer Control Program: CAD4-PC Version 1.5c, Delft Instruments X-ray Diffraction, Delft, The Netherlands, © 1994.

[11] Data were processed on a VAXStation 2004/166 (Open VMS/Alpha V6.2), with the program XCAD4B and with the commercial package SHELXTL Release 5.05/VMS, Siemens Analytical X-ray Instruments, Inc., Madison, WI, © 1996.

[12] G.M. Sheldrick, *Shelxl93*: FORTRAN-77 Program for the Refinement of Crystal Structures from Diffraction Data, University of Göttingen, 1993.

[13] J. Forniés, F. Martínez, R. Navarro and E.P. Urriolabeitia, *J. Organomet. Chem., 495* (1995) 185.

[14] J.A. Potenza, L. Zyontz, J. San Fillipo, Jr. and R.A. Lalancette, *Acta Crystallogr., Sect. B, 34* (1978) 2624.

[15] J. Vicente, M.D. Bermúdez, M.P. Carrillo and P.G. Jones, *J. Organomet. Chem., 456* (1993) 305.

[16] A.F. Wells, *Structural Inorganic Chemistry*, Oxford University Press, London, 5th edn., 1984, p. 922.